

High-performance Kernel Machines with Implicit Distributed Optimization and Randomization

Vikas Sindhwani*

Google Research

and

Haim Avron

IBM T.J. Watson Research Center

April 17, 2015

Abstract

We propose a framework for massive-scale training of kernel-based statistical models, based on combining distributed convex optimization with randomization techniques. Our approach is based on a block-splitting variant of the Alternating Directions Method of Multipliers, carefully reconfigured to handle very large random feature matrices under memory constraints, while exploiting hybrid parallelism typically found in modern clusters of multicore machines. Our high-performance implementation supports a variety of statistical learning tasks by enabling several loss functions, regularization schemes, kernels, and layers of randomized approximations for both dense and sparse datasets, in an extensible framework. We evaluate our implementation on large-scale model construction tasks, and provide a comparison against existing sequential and parallel libraries.

Keywords: big-data, scalability, kernel methods, statistical computations

*The authors gratefully acknowledge the support from XDATA program of the Advanced Research Projects Agency (DARPA), administered through Air Force Research Laboratory contract FA8750-12-C-0323

1 Introduction

A large class of supervised machine learning models are trained by solving optimization problems of the form,

$$f^* = \operatorname{argmin}_{f \in \mathcal{H}} \frac{1}{n} \sum_{i=1}^n V(\mathbf{y}_i, f(\mathbf{x}_i)) + \lambda r(f), \quad (1.1)$$

where,

- $\{(\mathbf{x}_i, \mathbf{y}_i)\}_{i=1}^n$ is a training set with n labeled examples, with inputs $\mathbf{x} \in \mathcal{X} \subset \mathbb{R}^d$ and associated target outputs $\mathbf{y} \in \mathcal{Y} \subset \mathbb{R}^m$;
- \mathcal{H} is a hypothesis space of functions mapping the input domain (a subset of \mathbb{R}^d) to the output domain (another subset of \mathbb{R}^m), over which the training process estimates a functional dependency $f^*(\cdot)$ by optimizing an objective function;
- $V(\cdot, \cdot)$ is a convex loss function which measures the discrepancy between “ground truth” and model prediction;
- $r(\cdot)$ is a convex regularizer that penalizes models according to their complexity, in order to prevent overfitting. The regularization parameter λ balances the classic tradeoff between data fitting and complexity control, which enables generalization to unseen test data.

One prevalent setting is that of a large training set (big n), with high-dimensional inputs and outputs. In such a setting, it is often relatively easier to solve (1.1) if we impose strong structural constraints on the model, e.g. by requiring \mathcal{H} to be linear, or severely restricted it in terms of sparsity or smoothness. However, it is now well appreciated among practitioners, that imposing such strong structural constraints on the model upfront often limits, both theoretically and empirically, the potential of big data in terms of delivering higher accuracy models. When strong constraints are imposed, data tends to exhausts the statistical capacity of the model causing generalization performance to quickly saturate.

As a consequence, practitioners are increasingly turning to highly nonlinear models with millions of parameters, or even infinite-dimensional models, that need to be estimated on very large datasets (see Hinton et al. (2012); Taigman et al. (2014); Krizhevsky et al. (2012); Socher et al. (2013); Huang et al. (2014)), often with carefully designed domain-dependent loss functions and regularizers. This trend, exemplified by the recent success of deep learning techniques, necessitates co-design at the intersection of statistics, numerical optimization and high performance computing. Indeed, highly scalable algorithms and implementations play a pivotal role in this setting as enablers of rapid experimentation of statistical techniques on massive datasets to gain better understanding of their ability to

truly utilize "big data", which, in turn, informs the design of even more effective statistical algorithms.

Kernel methods (see Schlkopf and Smola (2001)) constitute a mathematically elegant framework for general-purpose infinite-dimensional non-parametric statistical inference. By providing a principled framework to extend classical linear statistical techniques to non-parametric modeling, their applications span the entire spectrum of statistical learning: nonlinear classification, regression, clustering, time-series analysis, sequence modeling (Song et al. (2013)), dynamical systems (Boots et al. (2013)), hypothesis testing (Harchaoui et al. (2013)), causal modeling (Zhang et al. (2011)) and others.

The central object in kernel methods is a kernel function $k(\mathbf{x}, \mathbf{x}')$ defined on the input domain \mathcal{X} . This kernel function defines a suitable hypothesis space of functions \mathcal{H}_k with which (1.1) can be instantiated, and turned into a finite dimensional optimization problem. However, training procedures derived directly in this manner scale poorly, having training time that is cubic in n and storage that is quadratic in n , with limited opportunities for parallelization. This poor scalability poses a significant barrier for the use of kernel methods in big data applications. As such, with the growth in data across a multitude of applications, scaling up kernel methods Bottou et al. (2007) has acquired renewed and somewhat urgent significance.

In this work, we develop a highly scalable algorithmic framework and software implementation for kernel methods, for distributed-memory computing environments. Our framework combines two recent algorithmic techniques: randomized feature maps and distributed optimization method based on the Alternating Directions Method of Multipliers (ADMM) described by Boyd et al. (2011). This framework orchestrates local models estimated on a subset of examples and random features, towards a unified solution. Our approach builds on the block-splitting ADMM framework proposed by Parikh and Boyd (2014), but we carefully reorganize its update rules to extract much greater efficiency. Our framework is designed to be highly modular. In particular, one needs to only supply certain proximal operators associated with a custom loss function and the regularizer. Our ADMM wrapper can then immediately instantiate a solver for (1.1) for a variety of choices of kernels and learning tasks.

We benchmark our implementation in both high-performance computing environments as well as commodity clusters. Results indicate that our approach is highly scalable in both settings, and is capable of returning state-of-the-art performance in machine learning tasks. Comparisons against sequential and parallel libraries for Support Vector Machines shows highly favorable accuracy-time tradeoffs for our approach.

We acknowledge that the two main technical ingredients (namely, randomized feature maps and block splitting ADMM) of our paper are both based on known influential techniques. However, their combination in our framework is entirely novel and motivated by our empirical observations on real-world problems where it became evident that a carefully customized distributed solver was necessary to push the random features technique to its limits. By using a block splitting ADMM strategy on an implicitly defined (and partitioned) feature-map expanded matrix, which is repeatedly computed on the fly, we are able to control memory consumption and handle extremely large data dense matrices that arise due to both very large number of examples as well as random features. We stress that our combination requires modifying the block-splitting ADMM iterations in order to avoid memory consumption from becoming excessive very quickly. As we show in the experimental section, this leads to a scalable solver that bears fruit empirically.

The code is freely available for download and use as part of the libSkylark library(<http://xdata-skylark.github.io/libskylark/>).

The rest of this article is organized as follows. In section 2 we provide a brief background on various technical elements of our algorithm. In section 3 we describe the proposed algorithm. In section 4 we discuss the role of the random feature transforms in our algorithm. In section 5 we report experimental results on two widely used machine learning datasets: MNIST (image classification) and TIMIT (speech recognition). We finish with some conclusions in section 6.

2 Technical Background

In this section we provide a brief background on various technical elements of our algorithm.

2.1 Kernel Methods and Their Scalability Problem

We start with a brief description of kernel methods. A kernel function, $k : \mathcal{X} \times \mathcal{X} \mapsto \mathbb{R}$, is defined on the input domain $\mathcal{X} \subset \mathbb{R}^d$. This kernel function *implicitly* defines a hypothesis space of functions – the Reproducing Kernel Hilbert Space \mathcal{H}_k . The hypothesis space \mathcal{H}_k is also equipped with a norm $\|\cdot\|_k$ which acts as a natural candidate for the regularizer, i.e. $r(f) = \|f\|_k^2$. \mathcal{H}_k is then used to instantiate the learning problem (1.1) with $\mathcal{H} = \mathcal{H}_k$.

The attractiveness of using \mathcal{H}_k as the hypothesis space in (1.1) stems from the Representer Theorem (see Wahba (1990)), which guarantees that the solution admits the following

expansion (for each coordinate $f_j(\cdot)$ of the vector valued function $f^*(\cdot)$ in (1.1)),

$$f_j^*(\mathbf{x}) = \sum_{i=1}^n \alpha_{ji} k(\mathbf{x}, \mathbf{x}_i), j = 1 \dots m . \quad (2.1)$$

The expansion (2.1) is then used to turn (1.1) to a finite dimensional optimization problem, which can be solved numerically.

Consider, for example, the solution of (1.1) for the square loss objective $V(\mathbf{y}, \mathbf{y}) = \|\mathbf{y} - \mathbf{t}\|_2^2$. Plugging the expansion (2.1) into (1.1), the coefficients $\alpha_{ij}, j = 1 \dots m, i = 1 \dots, n$ can be found by solving the following linear system,

$$(\mathbf{K} + n\lambda\mathbf{I}_n) \alpha = \mathbf{Y}, \quad (2.2)$$

where $\mathbf{Y} \in \mathbb{R}^{n \times m}$ with row i equal to \mathbf{y}_i , \mathbf{K} is the $n \times n$ Gram matrix given by $\mathbf{K}_{ij} = k(\mathbf{x}_i, \mathbf{x}_j)$, and $\alpha \in \mathbb{R}^{n \times m}$ contains the coefficients α_{ij} . Problem (1.1) with other loss functions ($V(\cdot, \cdot)$), and “kernelization” of other linear statistical learning algorithms gives rise to a whole suite of statistical modeling techniques.

For a suitable choices of a kernels, the hypothesis space \mathcal{H}_k can be made very rich, thus implying very strong non-parameteric modeling capabilities, while still allowing the solution of (1.1) via numerical optimization. However, there is a steep price in terms of scalability. Consider, again, the solution of (1.1) for the squared loss. As \mathbf{K} is typically dense, solving (2.2) using a direct method incurs a $\Theta(n^3 + n^2(d + m))$ time complexity, and $\Theta(n^2)$ storage complexity. Once α is found, evaluating $f^*(\cdot)$ on new data point requires $\Theta(n(d + m))$. This training and test time complexity becomes unappealing when n is large.

2.2 Randomized Kernel Methods

Randomized kernel methods, pioneered by Rahimi and Recht (2007), has recently emerged as a key algorithmic device with which to dramatically accelerate the training of kernel methods via a linearization mechanism. To help understand the benefits of linearization, let us first compare the complexity of kernel methods on the square loss function, to the complexity of solving (1.1) in a linear hypothesis space

$$\mathcal{H}_l = \{f_{\mathbf{W}} : \mathbf{W} \in \mathbb{R}^{d \times m}, f_{\mathbf{W}}(\mathbf{x}) = \mathbf{W}^T \mathbf{x}\} .$$

With $\mathcal{H} = \mathcal{H}_l$, problem (1.1) reduces to solving the following ridge regression problem

$$\mathbf{W}^* = \operatorname{argmin}_{\mathbf{W} \in \mathbb{R}^{d \times m}} \frac{1}{n} \|\mathbf{X}\mathbf{W} - \mathbf{Y}\|_{fro}^2 + \lambda \|\mathbf{W}\|_{fro}^2,$$

where $\mathbf{X} \in \mathbb{R}^{n \times d}$ has row i equal to \mathbf{x}_i . Using classical direct methods, this problem can be solved in $\Theta(nd^2 + ndm + d^2m)$ operations, using $\Theta(nd)$ memory and requiring only $\Theta(dm)$ for evaluating $f^*(\cdot)$. The linear dependence on n (the “big” dimension) is much more attractive for large-scale problems. Furthermore, recently Demmel et al. (2012) showed that distributed implementations of key linear algebra kernels can be made communication efficient; we also note that the running time can be improved by using more modern algorithms based on randomized preconditioning (see Avron et al. (2010); Meng et al. (2014)). Thus, while \mathcal{H}_l is a weaker hypothesis space from a statistical modeling point of view, is much more attractive from a computational point of view.

Randomized kernel methods linearize \mathcal{H}_k by constructing an *explicit* feature mapping $\mathbf{z} : \mathbb{R}^d \mapsto \mathbb{R}^s$ such that $k(\mathbf{x}, \mathbf{y}) \approx \mathbf{z}(\mathbf{x})^T \mathbf{z}(\mathbf{y})$. We now solve (1.1) on $\mathcal{H}_{k,l}$ instead of \mathcal{H}_k , where

$$\mathcal{H}_{k,l} = \{f_{\mathbf{W}} : \mathbf{W} \in \mathbb{R}^{s \times m}, f_{\mathbf{W}}(\mathbf{x}) = \mathbf{W}^T \mathbf{z}(\mathbf{x})\}.$$

This is a linear regression problem that can be solved more efficiently. In particular, returning to the previous example with squared loss and regularizer $r(f_{\mathbf{W}}) = \|\mathbf{W}\|_{fro}^2$, the problem reduces to solving

$$\mathbf{W}^* = \operatorname{argmin}_{\mathbf{W} \in \mathbb{R}^{s \times m}} \frac{1}{n} \|\mathbf{Z}\mathbf{W} - \mathbf{Y}\|_{fro}^2 + \lambda \|\mathbf{W}\|_{fro}^2,$$

where $\mathbf{Z} \in \mathbb{R}^{n \times s}$ has row i equal to $\mathbf{z}(\mathbf{x}_i)$.

In general form, after selecting some $\mathbf{z}(\cdot)$ (a choice that is guided by the kernel $k(\cdot, \cdot)$ we want to use), we are faced with solving the problem

$$\operatorname{argmin}_{\mathbf{W} \in \mathbb{R}^{s \times m}} \frac{1}{n} \sum_{i=1}^n V(\mathbf{y}_i, \mathbf{W}^T \mathbf{z}_i) + \lambda r(\mathbf{W}) \tag{2.3}$$

where $\mathbf{z}_i = \mathbf{z}(\mathbf{x}_i)$. This technique relies on having a good approximation to $k(\cdot, \cdot)$ with moderate sizes of s , and having a cheap mechanism to generate the random feature matrix \mathbf{Z} from \mathbf{X} .

Randomized feature maps have proven to be very effective in extending the reach of kernel methods to larger datasets, e.g. on classical speech recognition datasets Huang et al. (2014). However, it has also been observed that in order to build state-of-the-art models

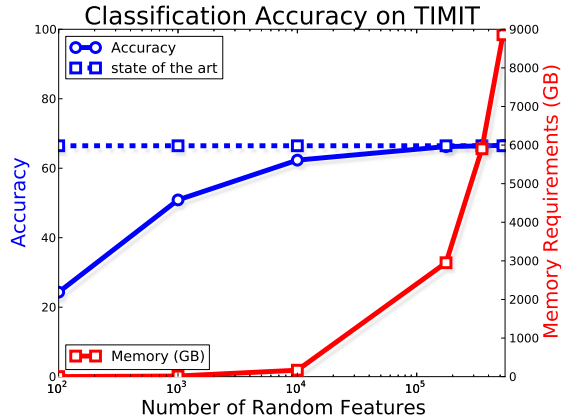


Figure 2.1: Performance of Randomized Kernel Methods. The largest model is trained on a supercomputer (BlueGene/Q), on an 8.7 terabyte dataset using implicit distributed optimization methods implemented in this paper for high-performance computing environments.

in applications of interest, a very large number of random features are needed (very large s). This is illustrated in Figure 2.1, which examines the use of (2.3) in a speech recognition application. This large number of features is challenging from a numerical optimization point of view. For example, the transformed data matrix \mathbf{Z} (whose rows are $\mathbf{z}(\mathbf{x}_i)$) now requires several terabytes of data, even though the original data matrix \mathbf{X} does not require too much storage.

2.3 Distributed Convex Optimization with ADMM

This section reviews distributed optimization using variants of the Alternating Direction Method of Multipliers (ADMM) described by Boyd et al. (2011).

Informally speaking, one may take the following heuristic approach for building statistical models using big datasets on distributed memory compute environments: partition the data between nodes, build a local models in each node, and generate a global model using some combination mechanism (e.g. averaging over the ensemble of local models). ADMM as applied to statistical learning problems follows a similar pattern, in that it orchestrates the estimation of the local models in the presence of a global model as prior. The appeal of ADMM is that it decomposes the problem into a set of proximal and projection operators which are computational patterns that repeat across a variety of settings. Thus, ADMM can be seen as a meta-algorithm, in which the user needs to only implement a small set of operators required to instantiate their problem, and ADMM as a wrapper takes care of

distributing the computation.

More concretely, ADMM solves optimization problems of the general form,

$$\begin{aligned} & \underset{\mathbf{x} \in \mathbb{R}^n, \mathbf{z} \in \mathbb{R}^m}{\operatorname{argmin}} f(\mathbf{x}) + g(\mathbf{z}) \\ & \text{subject to : } \mathbf{Ax} + \mathbf{Bz} = \mathbf{c} \end{aligned} \quad (2.4)$$

In this form, the objective function splits over convex functions f, g involving separate variables, tied via a linear constraint where $\mathbf{A} \in \mathbb{R}^{p \times n}, \mathbf{B} \in \mathbb{R}^{p \times m}, \mathbf{c} \in \mathbb{R}^p$. ADMM update rules are derived via Gauss-Seidel updates (cyclic coordinate descent) on the augmented Lagrangian,

$$L_\rho(\mathbf{x}, \mathbf{z}, \tilde{\boldsymbol{\nu}}) = f(\mathbf{x}) + g(\mathbf{z}) + \tilde{\boldsymbol{\nu}}^T (\mathbf{Ax} + \mathbf{Bz} - \mathbf{c}) + \frac{\rho}{2} \|\mathbf{Ax} + \mathbf{Bz} - \mathbf{c}\|_2^2 ,$$

resulting in the following iterations,

$$\mathbf{x}^{(j+1)} = \underset{\mathbf{x} \in \mathbb{R}^n}{\operatorname{argmin}} L_\rho(\mathbf{x}, \mathbf{z}^{(j)}, \tilde{\boldsymbol{\nu}}^{(j)}) \quad (2.5)$$

$$\mathbf{z}^{(j+1)} = \underset{\mathbf{z} \in \mathbb{R}^m}{\operatorname{argmin}} L_\rho(\mathbf{x}^{(j+1)}, \mathbf{z}, \tilde{\boldsymbol{\nu}}^{(j)}) \quad (2.6)$$

$$\tilde{\boldsymbol{\nu}}^{(j+1)} = \tilde{\boldsymbol{\nu}}^{(j)} + \rho (\mathbf{Ax}^{(j+1)} + \mathbf{Bz}^{(j+1)} - \mathbf{c}) \quad (2.7)$$

where $\rho > 0$ is the ADMM penalty parameter and $\tilde{\boldsymbol{\nu}}$ are dual variables associated with the constraint.

A generic constrained convex optimization problem,

$$\underset{\mathbf{x} \in \mathbb{R}^d}{\operatorname{argmin}} f(\mathbf{x}) \quad \text{subject to } \mathbf{x} \in \mathcal{C} \quad (2.8)$$

can be cast in ADMM form as,

$$\underset{\mathbf{x}, \mathbf{z}}{\operatorname{argmin}} f(\mathbf{x}) + \mathbb{I}_{\mathcal{C}}(\mathbf{z}) \quad \text{subject to } \mathbf{x} = \mathbf{z} , \quad (2.9)$$

where $\mathbb{I}_{\mathcal{C}}(\mathbf{z})$ is 0 if $\mathbf{z} \in \mathcal{C}$ and $+\infty$ otherwise. Above, the objective function and the constraint are separated by variable splitting and a consensus constraint is added. The augmented Lagrangian for this problem is given by,

$$L_\rho(\mathbf{x}, \mathbf{z}, \boldsymbol{\nu}) = f(\mathbf{x}) + \mathbb{I}_{\mathcal{C}}(\mathbf{z}) + \boldsymbol{\nu}^T (\mathbf{x} - \mathbf{z}) + \frac{\rho}{2} \|\mathbf{x} - \mathbf{z}\|_2^2 .$$

Thus, the ADMM update equations for solving (2.9) are

$$\begin{aligned}
\mathbf{x}^{(j+1)} &= \operatorname{argmin}_{\mathbf{x} \in \mathbb{R}^n} \left[f(\mathbf{x}) + \mathbf{x}^T \tilde{\boldsymbol{\nu}}^{(j)} + \frac{\rho}{2} \|\mathbf{x} - \mathbf{z}^{(j)}\|_2^2 \right] \\
&= \operatorname{argmin}_{\mathbf{x} \in \mathbb{R}^n} \left[\frac{1}{\rho} f(\mathbf{x}) + \frac{1}{2} \left\| \mathbf{x} - \left(\mathbf{z}^{(j)} - \frac{\tilde{\boldsymbol{\nu}}^{(j)}}{\rho} \right) \right\|_2^2 \right] \\
\mathbf{z}^{(j+1)} &= \operatorname{argmin}_{\mathbf{z} \in \mathbb{R}^m} \left[\mathbb{I}_{\mathcal{C}}(\mathbf{z}) + \frac{\rho}{2} \left\| \mathbf{z} - \left(\mathbf{x}^{(j+1)} + \frac{\tilde{\boldsymbol{\nu}}^{(j)}}{\rho} \right) \right\|_2^2 \right] \\
\tilde{\boldsymbol{\nu}}^{(j+1)} &= \tilde{\boldsymbol{\nu}}^{(j)} + \rho (\mathbf{x}^{(j+1)} - \mathbf{z}^{(j+1)})
\end{aligned}$$

In order to rewrite these equations more compactly, it is useful to define the following operators.

Definition 1 (Proximity Operator) *The Proximity (or Prox) operator associated with a function $f : \mathbb{R}^d \mapsto \mathbb{R}$ is a map $\operatorname{prox}_f : \mathbb{R}^d \mapsto \mathbb{R}^d$ given by*

$$\operatorname{prox}_f[\mathbf{x}] = \operatorname{argmin}_{\mathbf{y} \in \mathbb{R}^d} \frac{1}{2} \|\mathbf{x} - \mathbf{y}\|_2^2 + f(\mathbf{y})$$

Definition 2 (Projection Operator) *The Projection operator associated with a convex constraint set \mathcal{C} is the map $\operatorname{proj}_{\mathcal{C}} : \mathbb{R}^d \mapsto \mathbb{R}^d$ given by*

$$\operatorname{proj}_{\mathcal{C}}[\mathbf{x}] = \operatorname{argmin}_{\mathbf{y} \in \mathcal{C}} \frac{1}{2} \|\mathbf{x} - \mathbf{y}\|_2^2$$

Hence, $\operatorname{proj}_{\mathcal{C}} = \operatorname{prox}_{\mathbb{I}_{\mathcal{C}}}$.

For a variety of common loss functions and regularizers, the proximal operator admits closed-form formulas, that can be computed using efficient algorithms.

In addition, we use the *scaled dual variables* $\boldsymbol{\nu}^{(j)} \equiv \rho^{-1} \tilde{\boldsymbol{\nu}}^{(j)}$. Together with the above we get the following update rules:

$$\begin{aligned}
\mathbf{x}^{(j+1)} &= \operatorname{prox}_{\frac{1}{\rho} f}[\mathbf{z}^{(j)} - \boldsymbol{\nu}^{(j)}] \\
\mathbf{z}^{(j+1)} &= \operatorname{proj}_{\mathcal{C}}[\mathbf{x}^{(j+1)} + \boldsymbol{\nu}^{(j)}] \\
\boldsymbol{\nu}^{(j+1)} &= \boldsymbol{\nu}^{(j)} + \mathbf{x}^{(j+1)} - \mathbf{z}^{(j+1)}
\end{aligned} \tag{2.10}$$

3 Distributed Learning with ADMM Block Splitting and Hybrid Parallelism

In this section we describe the proposed algorithm for solving (2.3). Psuedo-code is given as Algorithm 1. In the following, the matrix \mathbf{X}, \mathbf{Y} are the input of the algorithm, where \mathbf{X} has \mathbf{x}_i as row i , and \mathbf{Y}_i has \mathbf{y}_i as row i . The matrix \mathbf{Z} denotes the result of applying the random transform $\mathbf{z}(\cdot)$ to \mathbf{X} , that is row i of \mathbf{Z} is $\mathbf{z}(\mathbf{x}_i)$.

Our algorithm is geared towards the following setup:

- A distributed-memory computing environment comprising of a cluster of N compute nodes, with T cores per node. We assume that each node has M GB of RAM.
- The training data \mathbf{X}, \mathbf{Y} are distributed *by rows* across the nodes. This is a natural assumption in large-scale learning since rows have the semantics of data instances which are typically collected or generated in parallel across the cluster to begin with.
- \mathbf{X}, \mathbf{Y} fit in the aggregate distributed memory of the cluster, but are large enough that they cannot fit on a single node, and cannot be replicated in memory on multiple nodes.
- The matrix \mathbf{Z} does not fit in aggregate distributed memory because n and s are both simultaneously big. This assumption is motivated by empirical observations shown in Figure 2.1.
- The matrix \mathbf{Z} cannot be stored on disk because of space restrictions, or it can but the I/O cost of reading it by blocks in every iteration is more expensive than the cost of recomputing blocks of \mathbf{Z} on the fly from scratch as needed, respecting per-node memory constraints. Thus, our algorithm uses a transform operator \mathbb{T} which when applied to \mathbf{X}_i given a block id j , produces the output \mathbf{Z}_{ij} , i.e.,

$$\mathbb{T}[\mathbf{X}_i, j] = \mathbf{Z}_{ij}$$

This transform function is used to generate \mathbf{Z}_{ij} as needed in the optimization process, used and discarded in each iteration. The construction of these transform operators is discussed in Section 4.

Our algorithm is based on the block-splitting variant of ADMM described by Parikh and Boyd (2014), which is well suited for the target setup. This approach assumes the data matrix is partitioned by both rows and columns. Independent models are estimated on

each block in parallel and orchestrated by ADMM towards the solution of the optimization problem. In addition to the proximal and projection operators, this variant makes use of the following operator.

Definition 3 (Graph Projection Operator Over Matrices) *The Graph projection operator associated with an $n \times d$ matrix \mathbf{A} is the map $\text{proj}_{\mathbf{A}} : \mathbb{R}^{n \times k} \times \mathbb{R}^{d \times k} \mapsto \mathbb{R}^{n \times k} \times \mathbb{R}^{d \times k}$ given by,*

$$\begin{aligned} \text{proj}_{\mathbf{A}}[(\mathbf{Y}, \mathbf{X})] &= \underset{(\mathbf{V}, \mathbf{U})}{\text{argmin}} \frac{1}{2} \|\mathbf{V} - \mathbf{Y}\|_{fro}^2 + \frac{1}{2} \|\mathbf{U} - \mathbf{X}\|_{fro}^2, \\ &\text{subject to : } \mathbf{V} = \mathbf{A}\mathbf{U} \end{aligned}$$

where $\mathbf{Y}, \mathbf{V} \in \mathbb{R}^{n \times k}$, $\mathbf{X}, \mathbf{U} \in \mathbb{R}^{d \times k}$. The solution is given by:

$$\mathbf{U} = [\mathbf{A}^T \mathbf{A} + \mathbf{I}]^{-1} (\mathbf{X} + \mathbf{A}^T \mathbf{Y}) \quad (3.1)$$

$$\mathbf{V} = \mathbf{A}\mathbf{U} \quad (3.2)$$

Remark The above solution formula is computationally preferable when $d \ll n$. When d is larger, the solution formula may be rewritten in terms of an $n \times n$ linear system involving $\mathbf{A}\mathbf{A}^T$ instead (see Parikh and Boyd (2014)). However, the $d \ll n$ case is more relevant for our setting.

Our algorithm is derived by first logically block partitioning the matrix \mathbf{Z} into $R \times C$ blocks, where R and C denote row and column splitting parameters respectively. The matrices \mathbf{X} and \mathbf{Y} are row partitioned into R blocks, while \mathbf{W} is row partitioned into C blocks:

$$\begin{pmatrix} \mathbf{X}_1 \\ \vdots \\ \mathbf{X}_R \end{pmatrix} \rightarrow \begin{pmatrix} \mathbf{Z}_{11} & \mathbf{Z}_{12} & \dots & \mathbf{Z}_{1C} \\ \vdots & \vdots & \vdots & \vdots \\ \mathbf{Z}_{R1} & \mathbf{Z}_{R2} & \dots & \mathbf{Z}_{RC} \end{pmatrix}, \begin{pmatrix} \mathbf{Y}_1 \\ \vdots \\ \mathbf{Y}_R \end{pmatrix}, \begin{pmatrix} \mathbf{W}_1 \\ \vdots \\ \mathbf{W}_C \end{pmatrix} \quad (3.3)$$

We assume that $\mathbf{X}_i \in \mathbb{R}^{n_i \times m}$, $\mathbf{Y}_i \in \mathbb{R}^{n_i \times m}$, $\mathbf{W}_j \in \mathbb{R}^{s_j \times m}$, $\mathbf{Z}_{ij} \in \mathbb{R}^{n_i \times s_j}$ where $\sum_{i=1}^R n_i = n$ and $\sum_{j=1}^C s_j = s$.

We assume a distributed-memory setup in which R processes are invoked on $N \leq R$ nodes, with the processes distributed evenly among the nodes. Processes communicate using message-passing; in our implementation, using the MPI (Message Passing Interface) protocol. Each process owns a row index i , i.e. it holds in memory \mathbf{X}_i and \mathbf{Y}_i . In the notation, we use i as an identifier of the process. We assume process i spawns $t \leq T$ threads

that collectively own the parallel computation related to the C blocks of $\mathbf{Z}_{ij}, j = 1 \dots C$. Setting the values of t , R and C are configuration options of the algorithm, however it should always be the case that $t \times R \leq N \times T$, and it is advisable that $t \leq C$. For reasoning about the algorithm, it is useful to assume that n is a multiple of R and that s is a multiple of C , and that we set $n_i = \frac{n}{R}$ and $s_j = \frac{s}{C}$. In practice, n and s are usually not exact multiples of R and C , and there is an imbalance in the values of $\{n_i\}$ and $\{s_j\}$.

To interpret the block-splitting ADMM algorithm, it is convenient to setup the following semantics. Let $\mathbf{W}_{ij} \in \mathbb{R}^{s_j \times m}$ denote local model parameters associated with block \mathbf{Z}_{ij} . We require each local model to agree with the corresponding block of global parameters, i.e., $\mathbf{W}_{ij} = \mathbf{W}_j$. The partial output of the local model on the block \mathbf{Z}_{ij} is given by $\mathbf{O}_{ij} = \mathbf{Z}_{ij} \mathbf{W}_{ij} \in \mathbb{R}^{n_i \times m}$. The aggregate output across all the columns is $\mathbf{O}_i = \sum_{j=1}^C \mathbf{O}_{ij} = (\mathbf{Z}\mathbf{W})_i$. Let the set of n_i indices in the i^{th} row block be denoted by I_i . We denote the local loss measured by process i as,

$$l_i(\mathbf{O}_i) = \frac{1}{n} \sum_{j \in I_i} V(\mathbf{y}_j, \mathbf{o}_j), i = 1 \dots M$$

where $\mathbf{o}_j^T, j \in I_i$ are rows of the matrix \mathbf{O}_i . Similarly, we assume that the regularizer $r(\cdot)$ in (2.3) is separable over row blocks, i.e. $r(\mathbf{W}) = \sum_{j=1}^C r_j(\mathbf{W}_j)$ where $\mathbf{W}_j \in \mathbb{R}^{s_j \times m}$ is the conforming block of rows of \mathbf{W} . This assumption holds for l_2 regularization, i.e., $r_j(\mathbf{W}_j) = \|\mathbf{W}_j\|_{fro}^2$.

With the notation setup above, it is easy to see that (2.3) can be equivalently rewritten over blocks as follows,

$$\begin{aligned} & \underset{\mathbf{W} \in \mathbb{R}^{s \times k}}{\operatorname{argmin}} \sum_{i=1}^R l_i(\mathbf{O}_i) + \lambda \sum_{j=1}^C r_j(\mathbf{W}_j) + \sum_{i,j} \mathbb{I}_{\mathbf{Z}_{ij}}(\mathbf{O}_{ij}, \mathbf{W}_{ij}) \\ \text{subject to} \quad & \mathcal{C}_1 : \mathbf{W}_{ij} = \mathbf{W}_j, \quad \text{for } i = 1 \dots R, j = 1 \dots C \\ & \mathcal{C}_2 : \mathbf{O}_i = \sum_{j=1}^C \mathbf{O}_{ij} \quad \text{for } i = 1 \dots R \end{aligned} \tag{3.4}$$

with

$$\mathbb{I}_{\mathbf{Z}_{ij}}(\mathbf{O}_{ij}, \mathbf{W}_{ij}) = \begin{cases} 0 & \text{if } \mathbf{O}_{ij} = \mathbf{Z}_{ij} \mathbf{W}_{ij} \\ \infty & \text{otherwise.} \end{cases}$$

Viewed as a convex constrained optimization problem, one can follow the progression (2.8) to (2.10). This requires introducing new consensus variables $\overline{\mathbf{W}}_j, \overline{\mathbf{W}}_{ij}, \overline{\mathbf{O}}_i, \overline{\mathbf{O}}_{ij}$ corresponding to $\mathbf{W}_j, \mathbf{W}_{ij}, \mathbf{O}_i, \mathbf{O}_{ij}$ and associated dual variables $\boldsymbol{\mu}_j, \boldsymbol{\mu}_{ij}, \boldsymbol{\nu}_i, \boldsymbol{\nu}_{ij}$. Further-

more, the projection onto the constraint sets \mathcal{C}_1 and \mathcal{C}_2 turn out to have closed form averaging and exchange solutions. Parikh and Boyd (2014) note that $\boldsymbol{\nu}_{ij}$ can be eliminated since $\boldsymbol{\nu}_{ij}$ turns out to equal $-\boldsymbol{\nu}_i$ after the first iteration. Similarly, $\overline{\mathbf{W}}_{ij} = \overline{\mathbf{W}}_j$ and hence $\overline{\mathbf{W}}_{ij}$ can also be eliminated. These simplifications imply the final modified update equations derived by Parikh and Boyd (2014), which take the following form when applied to (3.4):

$$\begin{aligned} \mathbf{O}_i^{(j+1)} &= \text{prox}_{\frac{1}{\rho}l_i} \left[\overline{\mathbf{O}}_i^{(j)} - \boldsymbol{\nu}_i^{(j)} \right] \\ \mathbf{W}_j^{(j+1)} &= \text{prox}_{\frac{\lambda}{\rho}r_j} \left[\overline{\mathbf{W}}_j^{(j)} - \boldsymbol{\mu}_j^{(j)} \right] \\ (\mathbf{O}_{ij}^{(j+1)}, \mathbf{W}_{ij}^{(j+1)}) &= \text{proj}_{\mathbf{Z}_{ij}} \left[\overline{\mathbf{O}}_{ij}^{(j)} + \boldsymbol{\nu}_i^{(j)}, \overline{\mathbf{W}}_j^{(j)} - \boldsymbol{\mu}_{ij}^{(j)} \right] \end{aligned} \quad (3.5)$$

$$\begin{aligned} \overline{\mathbf{W}}_j^{(j+1)} &= \frac{1}{R+1} \left(\mathbf{W}_j^{(j+1)} + \sum_{i=1}^R \mathbf{W}_{ij}^{(j+1)} \right) \\ \overline{\mathbf{O}}_{ij}^{(j+1)} &= \mathbf{O}_{ij}^{(j+1)} + \frac{1}{C+1} \left(\mathbf{O}_i^{(j+1)} - \sum_{j=1}^C \mathbf{O}_{ij}^{(j+1)} \right) \end{aligned} \quad (3.6)$$

$$\overline{\mathbf{O}}_i^{(j+1)} = \sum_j \overline{\mathbf{O}}_{ij}^{(j+1)} \quad (3.7)$$

$$\begin{aligned} \boldsymbol{\mu}_j^{(j+1)} &= \boldsymbol{\mu}_j^{(j)} + \mathbf{W}_j^{(j+1)} - \overline{\mathbf{W}}_j^{(j+1)} \\ \boldsymbol{\mu}_{ij}^{(j+1)} &= \boldsymbol{\mu}_{ij}^{(j)} + \mathbf{W}_{ij}^{(j+1)} - \overline{\mathbf{W}}_j^{(j+1)} \\ \boldsymbol{\nu}_i^{(j+1)} &= \boldsymbol{\nu}_i^{(j)} + \mathbf{O}_i^{(j+1)} - \overline{\mathbf{O}}_i^{(j+1)} \end{aligned}$$

where i runs from 1 to R and j from 1 to C . In the above, ρ is the ADMM step-size parameter.

Unfortunately, this form is *not* scalable in our setting despite the high degree of parallelism in it. This is because a naive implementation of the algorithm requires each node/process to hold the C local matrices $\mathbf{O}_{ij}, \overline{\mathbf{O}}_{ij}$ for a total memory requirement which grows as $2n_i C m$. This can be quite substantial for moderate to large values of the product Cm since n_i is expected to still be large. As an example, if $C = 64$ (which is a representative number of hardware threads in current high-end supercomputer nodes), for a 100-class classification problem, the maximum number of examples that a node can hold before consuming 16-GB memory (a reasonable amount of node-memory) by just one of these variables alone, is barely 335,000. The presence of these variables conflicts with the need to increase C to reduce the memory requirements and increase parallelism for solving the Graph projection step (3.5). Fortunately, the materialization of these variables can also be avoided by noting the form of the solution of Graph projection and exploiting shared

memory access of variables across column blocks.

First, the variable $\overline{\mathbf{O}}_{ij}$ only contributes to a running sum in (3.7) and appears in the Graph projection step (3.5) (which requires the computation of the product $\mathbf{Z}_{ij}^T \overline{\mathbf{O}}_{ij}$). These steps, together with the update of $\overline{\mathbf{O}}_{ij}$ in (3.6) can be merged while eliminating each of the C variables, $\overline{\mathbf{O}}_{ij}$, as follows. We introduce an $s \times k$ variable $\mathbf{U}_i \in \mathbb{R}^{s \times m}$ and instead maintain $\mathbf{U}_{ij} = \mathbf{Z}_{ij}^T \mathbf{O}_{ij} \in \mathbb{R}^{s_j \times m}$. A single new variable $\Delta \in \mathbb{R}^{n_i \times m}$ tracks the value of $\mathbf{O}_i - \sum_{j=1}^C \mathbf{O}_{ij}$ which is updated incrementally as $\mathbf{O}_{ij} = \mathbf{Z}_{ij} \mathbf{W}_{ij}$. Thus, (3.6) implies the following update,

$$\mathbf{Z}_{ij}^T \overline{\mathbf{O}}_{ij} = \mathbf{U}_{ij} + \frac{1}{C+1} \mathbf{Z}_{ij}^T \Delta$$

which can be used in (3.8). The update in (3.7) can also be replaced with $\overline{\mathbf{O}}_i = \frac{1}{C+1} \sum_{j=1}^C \mathbf{O}_{ij} + \frac{C}{C+1} \mathbf{O}_i$. Thus the updates can be reorganized so that the algorithm is much more memory efficient, while still requiring no more than one (expensive) call to the random features transform function \mathbb{T} . The price is that the running sum in (3.7) can not be done in parallel, so its depth is now linear in C instead of logarithmic.

The graph projection step (3.5) requires the computation of (3.1) with $\mathbf{A} = \mathbf{Z}_{ij}$, i.e. (dropping the iteration indices to reduce clutter),

$$\mathbf{W}_{ij} = \mathbf{Q}_{ij} [\overline{\mathbf{W}}_j - \boldsymbol{\mu}_{ij} + \mathbf{Z}_{ij}^T (\overline{\mathbf{O}}_{ij} + \boldsymbol{\nu}_i)] \quad (3.8)$$

$$\mathbf{O}_{ij} = \mathbf{Z}_{ij} \mathbf{W}_{ij} \quad (3.9)$$

where

$$\mathbf{Q}_{ij} = [\mathbf{Z}_{ij}^T \mathbf{Z}_{ij} + \mathbf{I}]^{-1}. \quad (3.10)$$

The matrix \mathbf{Q}_{ij} (or the Cholesky factors of the inverse above) can be cached during the first iteration and reused for faster solves in subsequent iterations. The cache requires $O(\sum_{j=1}^C s_j^2)$ memory, i.e. $O(\frac{s^2}{C})$ memory if $s_j = \frac{s}{C}$. Thus, increasing the column splitting reduces the memory footprint. It also reduces the total number of floating-point operations required for (3.8), to $O(\frac{s^2}{C})$.

The final update equations are the ones used in Algorithm 1, which also indicates which steps can be parallelized over multiple threads. A more schematic (but less formal) illustration is given in Figure 3.1.

Modularity. Note that the loss function and the regularizer only enter the ADMM updates via their proximal operator. Thus, one needs to only specify a sequential proximal operator function, for the ADMM wrapper to immediately yield a parallel solver. While

Algorithm 1 BlockADMM($\mathbf{X}, \mathbf{Y}, l, r, \mathbb{T}$)

1: **Setup:** The algorithm is run in a SIMD manner on R nodes. In each node, i is the node-id associated with the node. Node i also has access to the part of the data associated with it ($\mathbf{X}_i, \mathbf{Y}_i$), part of the loss function associated with it (l_i), the regularizer (r) and the randomized transform (\mathbb{T}).

2: **Initialize to zero:** $\mathbf{O}, \bar{\mathbf{O}}, \nu, \bar{\Delta} \in \mathbb{R}^{n_i \times m}$, $\bar{\mathbf{W}}, \mathbf{W}', \mu', \mu, \mathbf{U} \in \mathbb{R}^{s \times m}$, $\mathbf{W} \in \mathbb{R}^{s \times m}$

3: **for** iter = 1 ... max **do**

4: $\mathbf{O} \leftarrow \text{prox}_{\frac{1}{\rho} l_i} [\bar{\mathbf{O}} - \nu]$ {can use multiple threads to compute faster}

5: **if** $i = 0$ **then**

6: **in parallel, for** $j = 1, \dots, C$ **do:** $\mathbf{W}_j \leftarrow \text{prox}_{\frac{\Delta}{\rho} r} [\bar{\mathbf{W}}_j - \mu_j]$

7: **BROADCAST**($\bar{\mathbf{W}}$)

8: **else**

9: **RECEIVE**($\bar{\mathbf{W}}$)

10: **end if**

11: $\Delta \leftarrow \mathbf{O}$

12: $\bar{\mathbf{O}} \leftarrow \frac{C}{C+1} \mathbf{O}$

13: **in parallel, for** $j = 1, \dots, C$ **do**

14: {subindexing a matrix by j denotes the j th row-block of the matrix}

15: $\mathbf{Z}_{ij} \leftarrow \mathbb{T}[\mathbf{X}_i, j]$

16: **if** iter = 0, setup cache: \mathbf{Q}_{ij} according to (3.10)

17: $\mathbf{A} \leftarrow \frac{1}{C+1} \mathbf{Z}_{ij}^T \bar{\Delta}$

18: $\mathbf{W}'_j \leftarrow \mathbf{Q}_{ij} [\bar{\mathbf{W}}_j - \mu'_j + \mathbf{U}_j + \mathbf{A}]$

19: $\mathbf{O}' \leftarrow \mathbf{Z}_{ij} \mathbf{W}'_j$

20: **in critical section:** $\Delta \leftarrow \Delta - \mathbf{O}'$

21: $\mathbf{U}_j \leftarrow \mathbf{Z}_{ij}^T \mathbf{O}'$

22: **in critical section:** $\bar{\mathbf{O}} \leftarrow \bar{\mathbf{O}} + \frac{1}{C+1} \mathbf{O}'$

23: $\mu'_j \leftarrow \mu'_j + \mathbf{W}'_j - \bar{\mathbf{W}}_j$

24: **end for**

25: $\bar{\Delta} \leftarrow \Delta$

26: **if** $i = 0$ **then**

27: $\mu \leftarrow \mu + \mathbf{W} - \bar{\mathbf{W}}$

28: $\bar{\mathbf{W}} \leftarrow \frac{1}{R+1} \text{REDUCE}(\mathbf{W}')$

29: $\bar{\mathbf{W}} \leftarrow \bar{\mathbf{W}} + \frac{1}{R+1} \mathbf{W}$

30: **else**

31: **SEND-TO-ROOT**(\mathbf{W}')

32: **end if**

33: $\nu \leftarrow \nu + \mathbf{O} - \bar{\mathbf{O}}$

34: **end for**

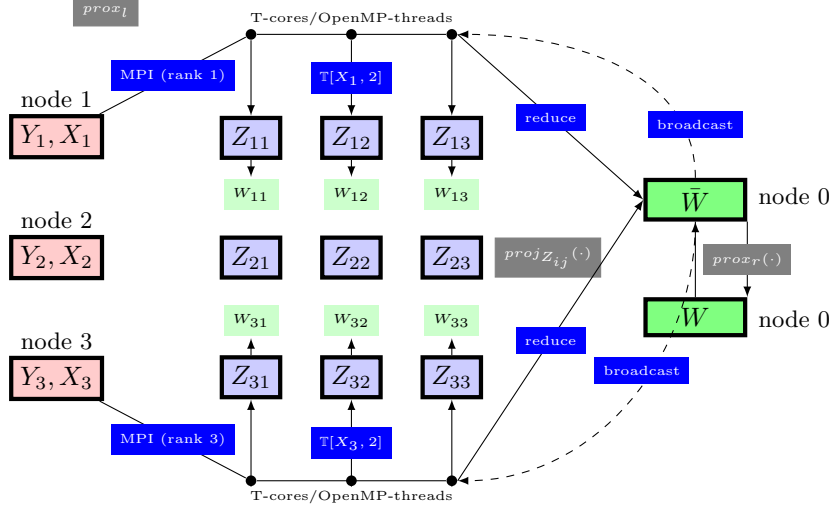


Figure 3.1: Schematic description of the proposed algorithm. The input data is split between different nodes (3 in the figure). Each node generates updated models based on the data it sees. The models are averaged on node 0 (using a reduce operation) and a consensus model is created and distributed. The update of the model on each node is done in parallel using OpenMP threads.

our current implementation supports squared loss, l_1 loss, hinge loss and multinomial logistic loss, our experiments focus on the hinge loss case that corresponds to the support vector machine (SVM) model. Boyd et al. (2011) show that the proximal operator for the hinge loss has a closed form solution.

Memory Requirements. Assuming $s_j = \frac{s}{C}$ and $n_i = \frac{n}{R}$, the total memory requirements per process (as reflected by counting the amount of floating point numbers) can be computed as follows:

$$\underbrace{\frac{4nm}{R}}_1 + \underbrace{5sm}_2 + \underbrace{\frac{nd}{R} + \frac{nm}{R}}_3 + \underbrace{\frac{tns}{RC}}_4 + \underbrace{\frac{tsm}{C} + \frac{nmt}{R} + \frac{nm}{R}}_5 + \underbrace{\frac{s^2}{C}}_6$$

where the terms can be associated with the variables: (1) $(\mathbf{O}, \bar{\mathbf{O}}, \nu, \bar{\Delta})$, (2) $\bar{\mathbf{W}}, \mathbf{W}'\boldsymbol{\mu}', \boldsymbol{\mu}, \mathbf{U}$; (3) the data $\mathbf{X}_i, \mathbf{Y}_i$; (4) the materialization of the block \mathbf{Z}_{ij} across the t threads; (5) private and shared temporary variables $(\mathbf{A}, \mathbf{O}')$ and Δ respectively, needed for the loop starting at step 13; and (6) the factorization cache.

If R is a multiple of N , then the total memory requirements per node are

$$\frac{4nm}{N} + \frac{5smR}{N} + \frac{nd}{N} + \frac{nm}{N} + \frac{tns}{CN} + \frac{tsmR}{CN} + \frac{nmt}{N} + \frac{nm}{N} + \frac{s^2R}{CN} \quad (3.11)$$

Equation (3.11) has a term that is quadratic in s , which is undesirable. However, the dependence is $O(s^2/C)$, where C is under the control of the user. Thus, increasing the column splitting C , reducing the number of threads t and reducing the ratio R/N provide knobs with which to satisfy memory constraints. In particular, we advocate having $C = O(s/d)$ and $R = N$. Choosing $C = \kappa \frac{s}{d}$ (with κ a parameter) and $R = N$, the memory requirements simplify to:

$$\frac{nm}{N} (t + 6) + \frac{nd}{N} + 5sm + \frac{1}{\kappa} \left(\frac{tnd}{N} + tmd + sd \right).$$

Note that forming \mathbf{Z} in memory, and then applying a linear method, requires at least $O(ns/N)$ memory per node. In contrast, with $C = O(s/d)$ our method requires only $O(nd/N)$, assuming that $s = O(n/N)$, $t = O(1)$, and $m \leq d \leq n$.

Computational Complexity. In terms of computation, the prox operator computation in steps 4 and 6 parallelize over multiple threads and have linear complexity. Assuming $R = N$, $s_j = \frac{s}{C}$ and $n_i = \frac{n}{N}$, the three dominant computational phases are:

- Cost of invoking the transform $\mathbb{T}[\mathbf{X}_i, j]$ in step 15, which tends to be the cost of right matrix multiplication of a random $d \times s_j$ matrix against \mathbf{X}_i , i.e. $O(\frac{nds}{CN})$. The depth is $O(\frac{nds}{tN})$. For certain transforms this can be accelerated as discussed in section 4.
- $O(\frac{nm}{N})$ cost per sum in steps 20 and 22, and a depth of $O(\frac{nmC}{N})$ due to the critical section.
- $O(\frac{s^2m}{C^2})$ cost of Graph Projection step 18, with depth $O(\frac{s^2m}{tC})$.
- $O(\frac{nsm}{CN})$ cost of matrix multiplications against blocks of \mathbf{Z} in steps 17, 19 and 21, with depth $O(\frac{nsmt}{tN})$.

Communication. The cost of broadcast/reduce operations in steps 7/9 and 28/31 costs grow as $O(sm \log N)$.

4 Randomized Kernel Maps

We now discuss the role of the random feature transforms $\mathbf{z}(\cdot)$ in our distributed solver. Since the initial work of Rahimi and Recht (2007), several alternative mappings have been suggested in the literature. These different mappings tradeoff the complexity of the transformation on dense/sparse vectors, kernel approximation, kernel choice, memory requirements, etc. Our algorithm encapsulates $\mathbf{z}(\cdot)$ and these choices via the operator \mathbb{T} , which is defined by $\mathbf{z}(\cdot)$; once $\mathbf{z}(\cdot)$ is fixed, it is treated as a black-box by our algorithm via \mathbb{T} as all other steps of the algorithm are the same.

This makes our algorithm highly modular, as it can operate on different kernels, and different kernel maps. The use of \mathbb{T} also encapsulates different treatment for sparse or dense input – as all kernel maps output dense vectors, different treatment of sparse and dense input appears solely in the application of \mathbb{T} (the blocks \mathbf{Z}_{ij} are treated as dense).

Given i and j , our algorithm assumes that it can compute $\mathbf{Z}_{ij} = \mathbb{T}[\mathbf{X}_i, j]$. Now, the rows of \mathbf{Z}_{ij} contain only some of the coordinates of applying $\mathbf{z}(\cdot)$ to the rows of \mathbf{X}_i . Most known schemes for constructing kernel maps, split naturally into blocks like this with no additional penalty. However, some schemes essentially need to compute the entire transformed vector in order to get the coordinates of choice. We overcome this in the following way. Given a known scheme for generating kernel maps, we construct the kernel map $\mathbf{z}(\cdot)$ as follows

$$\mathbf{z}(\mathbf{x}) = \frac{1}{\sqrt{s}} [\sqrt{s_1}\mathbf{z}_1(\mathbf{x}) \dots \sqrt{s_C}\mathbf{z}_C(\mathbf{x})]^T$$

where $\mathbf{z}_j : \mathbb{R}^d \mapsto \mathbb{R}^{s_j}$, $j = 1, \dots, C$ is a feature map generated independently. That is, we use of Monte-Carlo approximation. We can now set $\mathbb{T}[\mathbf{X}_i, j]$ to be result of applying $\mathbf{z}_j(\cdot)$ to the rows of \mathbf{X}_i and scaling them by $\sqrt{s_j/s}$

The primary feature map implemented in our solver is the Random Fourier Features technique. This the mapping suggested by Rahimi and Recht (2007). It is designed for the Gaussian kernel $k(\mathbf{x}, \mathbf{z}) = \exp(-\|\mathbf{x} - \mathbf{z}\|_2^2/2\sigma^2)$ (for some $\sigma \in \mathbb{R}$)¹. The mapping is $\mathbf{z}(\mathbf{x}) = \cos(\boldsymbol{\omega}^T \mathbf{x} + \mathbf{b})/\sqrt{s}$ where $\boldsymbol{\omega} \in \mathbb{R}^{d \times s}$ is drawn from an appropriately scaled Gaussian distribution, $\mathbf{b} \in \mathbb{R}^s$ is drawn from a uniform distribution on $[0, \pi)$, and the cosine function is applied entry-wise. For a dense input vector \mathbf{x} , the time to transform using $\mathbf{z}(\cdot)$ is $O(sd)$, and for a sparse input \mathbf{x} it is $O(s \text{nnz}(\mathbf{x}))$, where $\text{nnz}(\mathbf{x})$ is the number of non-zero entries in \mathbf{x} .

When applied to a group of inputs collected inside a matrix (as in generating \mathbf{Z}_{ij} from

¹The construction suggested by Rahimi and Recht (2007) actually spans a full family of shift-invariant kernels.

\mathbf{X}_{ij}), most of the operations can be done inside a single general matrix multiplication (GEMM), which gives access to highly tuned parallel basic linear algebra subprograms (BLAS) implementations.

Notice that naively representing $\mathbf{z}(\cdot)$ on a machine requires $O(sd)$ memory (storing the entries in ω), which can be rather costly. We avoid this by keeping an implicit representation in terms of the state of the pseudo random number generator, and generating parts of the ω on the fly, as needed.

Our solver also implements other feature maps: Fast Random Fourier Features (also called Fastfood) Le et al. (2013), Random Laplace Features Yang et al. (2014) and TensorSketch Pham and Pagh (2013). However, our experimental section is mainly focused on Random Fourier Features.

5 Experimental Evaluation

Datasets: We report experimental results on two widely used machine learning datasets: MNIST (image classification) and TIMIT (speech recognition). MNIST is a 10-class digit recognition problem with training set comprising of $n \approx 8.1M$ examples and a test set comprising of 10K instances. There are $d = 784$ features derived from intensities of 28×28 pixel images. TIMIT is 147-class phoneme classification problem with a training set comprising of $n \approx 2.2M$ examples and a test set comprising of 115,934 instances. The input dimensionality is $d = 440$.

Cluster Configuration: We report our results on two distributed memory computing environments: a BlueGene/Q rack (1,024 nodes, 16-cores per node and 4-way hyperthreading), and a 20-node commodity cluster TRILOKA with 8 cores per node. The latter is representative of typical cloud-like distributed environments, while the former is representative of traditional high-end high performance computing resources.

Default Parameters and Metrics: We report results with Gaussian kernels and Hinge Loss (SVMs). We use Random Fourier Feature maps (see Section 4), and store the input dataset using a dense matrix representations. We report speedups, running times for fixed number of ADMM iterations, and classification accuracy obtained on a test set.

5.1 Strong Scaling Efficiency

Strong scaling is defined as how the solution time varies with the number of processors for fixed total problem size. As such, in our setup, evaluation of strong scaling should be approached with caution: the standard notion of strong scaling generally assumes that parallelization accelerates a sequential algorithm, but does not change too much (or at all) the results and their quality. Thus, the focus is on the computational gains and communication overhead tradeoffs. This is not exactly the case for our setup. While it is possible to fix the amount of work in our algorithm by fixing n , d and the number of iterations, we are not guaranteed to provide results of the same quality as the number of row splits increase (i.e., as we use more processors).

ADMM guarantees only *asymptotic* convergence to the same solution, irrespective of data splitting. This introduces statistical tradeoffs since in practice, machine learning algorithms rarely attempt to find very high-precision solutions to the optimization problem, since the goal is to estimate a model that generalizes well, rather than solve an optimization problem (indeed, it can be rigorously argued that optimization error need not be reduced below statistical estimation errors, see Bottou and Bousquet (2007)). Increased row splitting implies that ADMM coordinates among a larger number of local models, each of which is statistically weaker, so we expect some slowdown of learning rate in a strong scaling regime. Thus, our experiments also evaluate how row splitting affects the classification accuracy.

Results of our strong scaling experiments are shown in Figure 5.1 and summarized in the following paragraphs.

MNIST: The number of random features is set to $100K$, and we use 200 column partitions. On TRILOKA we use $n = 200K$ while varying the number of processors from 1 to 20. Memory consumption (calculated using the analytical formula in Section 3) is about 6.2GB in the minimum configuration (one node). We observe nearly ideal speedup. On BG/Q we use $n = 250K$, and vary the number of nodes from 32 to 256. Memory consumption (calculated using the analytical formula in Section 3) is about 2.4GB in the minimum configuration (32 nodes). We measure speedup and parallel efficiency with respect to 32 nodes. We observe nearly ideal speedup on 64 nodes. With higher node counts the parallel efficiency starts to decline, but it is still very respectable (57%) on 256 nodes. The increased row splitting causes non-significant slowdown in learning rate.

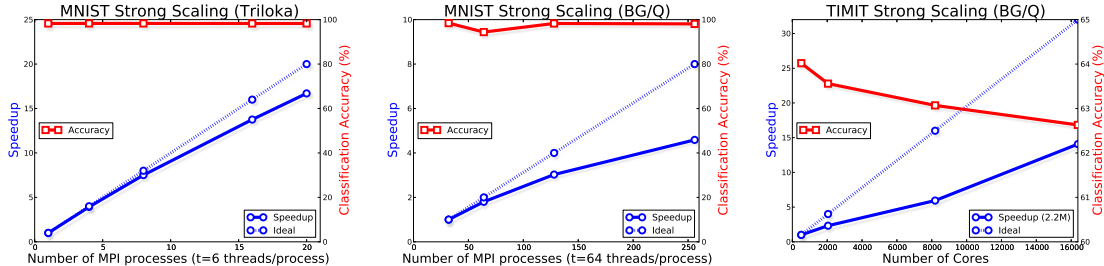


Figure 5.1: Strong-scaling experiments.

TIMIT: We use the entire dataset and experiment only on BG/Q. The number of random features is set to 176K, and we use 200 column partitions. Speedup is not far from linear, and parallel efficiency is 40% for 256 nodes. In terms of learning rate, accuracy curve declines and the slowdown is apparent, implying that more iterations are required to yield similar quality model.

5.2 Weak Scaling Efficiency

Weak scaling is defined as how the solution time varies with the number of processors for a fixed problem size per processor. Our algorithm is geared toward a weak scaling regime in which the number of random features and number of iterations stay constant, and the number of examples grows with the number of processors². This is a natural regime (but not the only one) for "big data" computation since it captures the case where more and more examples of equal size are collected over time. Contrary to a strong scaling regime, in such a regime we expect the classification accuracy to increase as more parallel resources are pulled in.

Results are reported in Figure 5.2. On TRILOKA, number of examples is increased at the rate of 10K examples per node. On BG/Q (MNIST only), the number of examples is increased at the rate of 250K per node. Results show nearly constant running time. In terms of improvement in classification accuracy, we see significant improvement of models trained on TRILOKA as the number of examples increase. The gains are modest for BG/Q runs since the baseline model trained on 250K examples already has high accuracy.

²Although we caution that there are non-trivial interaction between the various parameters, so in fact, one may want to increase the number of random features and number of iterations when more examples are used. However, exploring these interactions is not the scope of this article.

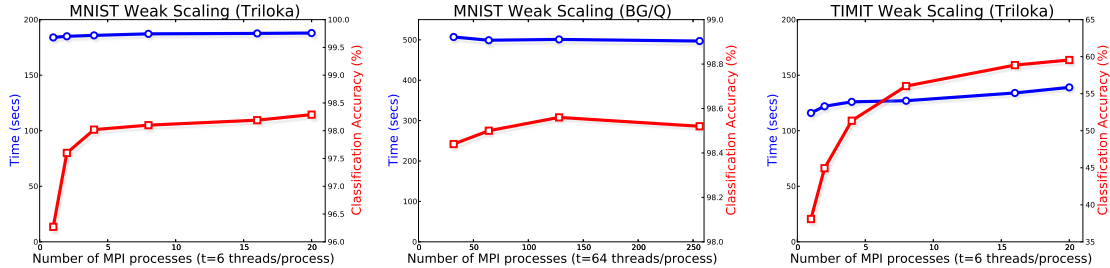


Figure 5.2: Weak Scaling experiments

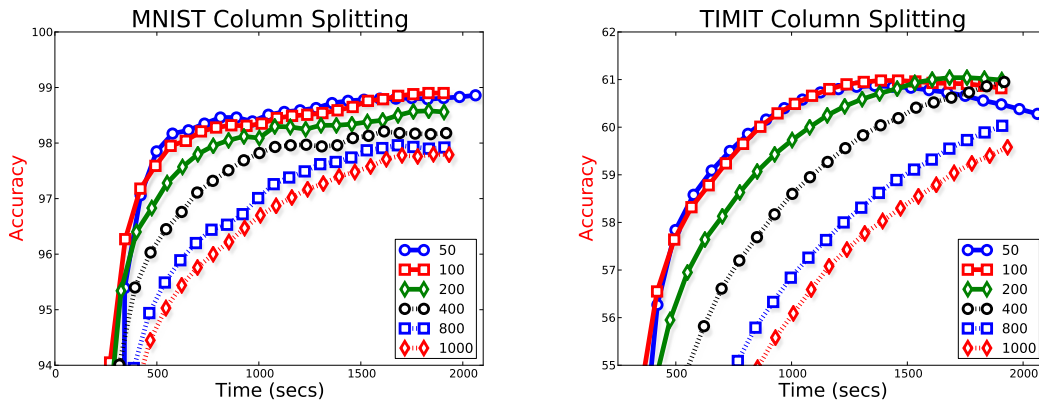


Figure 5.3: Effect of Column Splitting

5.3 Effect of Column Partitions

Figure 5.3 shows the effect of increasing the number of column splits, C , when using $100K$ random features for both MNIST and TIMIT. Increasing C reduces memory requirements and improves the running time of Graph projections. This comes with the tradeoff that the rate of learning per iteration can be significantly slowed, e.g. with $C = 1000$. At the same time, the plot shows that $C = 50, 100, 200$ perform similarly, and hence the optimization admits lower memory execution with little loss in terms of quality of the results.

As a rule of thumb, we advocate setting C to roughly s/d , since that ensures the ability to accommodate the memory requirements as long as the input matrix does not use more than $1/t$ of the available memory.

5.4 Performance Breakdown for Training Big Models

Table 5.1 shows the performance breakdown of a model learnt on the full TIMIT dataset, with $528K$ random features on BG/Q with 256 nodes. This model returns state-of-the-art

Table 5.1: Performance breakdown for training Big Models. Remark: the profiled steps are not disjoint (so percentages sum to more than 100%).

Step	Min Time	Max Time	Avg Time	Percentage
Communication (Steps 7/9, 28/31)	81	396	381	5%
Transform (Step 15)	2175	2185	2180	29.4%
Graph Projection Loop (Steps 13-24)	6464	6548	6512	88%
Proximal Operators (Steps 4,6)	0.19	0.21	0.20	0%
Barrier	0	55	54	0.7%
Prediction	417	501	453	6%
Total	7419	7419	7419	100%

accuracy (see Figure 2.1). Note that to materialize \mathbf{Z} explicitly 8.7 TB of memory is required. As Table 5.1 shows, the Graph projection loop, in particular the feature transformation step and the matrix multiplication against blocks of \mathbf{Z} , dominate the running time (which includes prediction on the test set at every iteration). The proximal operator costs is minimal because of closed form solutions that is embarrassingly parallel over multiple threads. The communication costs are also non-significant for reducing and broadcasting model parameters which in this case are buffers of size 0.6 GB. To reduce the overall time per iteration further, we plan to investigate a stochastic version of the algorithm where only a random subset of blocks are updated.

5.5 Comparison against Sequential and Parallel Solvers

Here we provide a sense of how our solvers compare with two other solvers.

In this section we compare our solver to existing solvers. In the first set of experiments we compare our solver with two other solvers for kernel SVM. The first one, LibSVM (see Chang and Lin (2011))³, is widely acknowledged to be the state-of-the-art sequential solver. The other one, PSVM (see Chang et al. (2007)), is an open source MPI-based parallel SVM code. PSVM computes in parallel a low-rank factorization of the Gram matrix via Incomplete Cholesky and then uses this factorization to accelerate a primal-dual interior point method for solving the SVM problem.

We compiled a multithreaded version of LibSVM. Since PSVM only supports binary classification, we created versions of MNIST and TIMIT by dividing their classes into a positive and negative class. A comparison is shown below for an SVM problem with Gaussian

³<http://www.csie.ntu.edu.tw/~cjlin/libsvm/>

Table 5.2: Comparison on MNIST-binary (200k)

	LibSVM	PSVM ($n^{0.5}$)	BlockADMM
Training Time	108720	194.15	178.82
Testing Time	169	8.45	1.63
Accuracy	98.51%	72.14%	97.55%

Table 5.3: Comparison on TIMIT-binary (100k)

	Libsvm	PSVM ($n^{0.5}$)	BlockADMM
Training Time	80355	47	42
Testing Time	1295	259	2.9
Accuracy	85.41%	73.1%	83.47%

kernels ($\sigma = 10$) and regularization parameter $\lambda = 0.001$. We use TRILOKA with 20 nodes and 6 cores. LibSVM, with its default optimization parameters, requires more than a day to solve the binary MNIST problem and about 22 hours to solve the binary TIMIT problem. The testing time is also significant particularly for TIMIT which has a large test set with more than 115K examples. The main reason for this slow prediction speed is that the number of support vectors found by LibSVM is not small: 15,667 for MNIST and 45,071 for TIMIT, making the evaluation of (2.1) computationally expensive. This problem is shared by PSVM though its prediction speed is faster due to parallel evaluation. However, PSVM runtimes rapidly increase with its rank parameter p . For $p = \sqrt{n}$ (advocated by Chang et al. (2007)), the estimated model provides a much worse accuracy-time tradeoff than our solver, which can work with much larger low-rank approximations that are computed locally and cheaply. On both datasets, our solver approaches the LibSVM classification accuracy.

In the second set of experiments, we examine how our solver compares to using a linear solver with a dataset preprocessed with random features. We use the Birds library Yang (2013), a distributed library for linear classification and regression. We use a reduced MNIST(200K examples) dataset and reduced TIMIT(100K examples) dataset, and instead of passing the dataset itself to Birds, we pass a dataset obtained by applying the random Fourier features transform to the original dataset. We use 30K random features for MNIST, and 10K random features for TIMIT. We use a total of 120-cores: 20 nodes and 6 threads per node for our solver, and 20 nodes and 6 tasks per node for Birds (Birds does not have hybrid parallel capabilities). We use Birds with hinge-loss and default parameters.

Table 5.4: Comparison to a distributed linear solver on a preprocessed dataset

	Birds		BlockADMM	
	Training Time	Accuracy	Training Time	Accuracy
MNIST-200K	754	97.58%	479	98.76%
TIMIT-100K	3333	46.7%	104	46.8%

Table 5.4 reports the results of this experiment, and the comparison to our solver using the same random features. Note that the running time of Birds does *not* include the time to apply the random feature transform. We see that our solver is much faster, and also attains higher accuracy.

We remark that the method of preprocessing a dataset with random features and applying a linear solver is not scalable. It requires holding the entire random feature matrix in memory, and this is memory-demanding. In contrast, our method never forms the entire random-feature matrix in memory, and thus has a much smaller memory footprint.

6 Conclusion

Our goal in this paper has been to resolve scalability challenges associated with kernel methods by using randomization in conjunction with distributed optimization. We noted that this combination leads to a class of problems involving very large implicit datasets. To handle such datasets in distributed memory computing environments where we also want to exploit shared memory parallelism, we investigate a block-splitting variant of the ADMM algorithm which is reorganized and adapted for our specific setting. Our approach is high-performance both in terms of scalability as well as in terms of statistical accuracy-time tradeoffs. The implementation supports various loss functions and is highly modular. We plan to investigate a stochastic version of our approach where only a random selection of blocks are updated in each iteration.

References

- Avron, H., Maymounkov, P., and Toledo, S. (2010). Blendenpik: Supercharging LAPACK’s least-squares solver. *SIAM J. Sci. Comput.*, 32(3):1217–1236.
- Boots, B., Gretton, A., and Gordon, G. J. (2013). Hilbert space embeddings of predictive

- state representations. In *Proc. 29th Intl. Conf. on Uncertainty in Artificial Intelligence (UAI)*.
- Bottou, L. and Bousquet, O. (2007). The tradeoffs of large-scale learning. In *Advances in Neural Information Processing Systems (NIPS)*.
- Bottou, L., Chapelle, O., DeCoste, D., and (Editors), J. W. (2007). *Large-scale Kernel Machines*. MIT Press.
- Boyd, S., Parikh, N., Chu, E., Peleato, B., and Eckstein, J. (2011). Distributed optimization and statistical learning via the alternating direction method of multipliers. *Foundations and Trends in Machine Learning.*, 3(1):1–122.
- Chang, C.-C. and Lin, C.-J. (2011). LIBSVM: A library for support vector machines. *ACM Trans. Intell. Syst. Technol.*, 2(3):27:1–27:27.
- Chang, E. Y., Zhu, K., Wang, H., Bai, H., Li, J., Qiu, Z., and Cui, H. (2007). PSVM: Parallelizing support vector machines on distributed computers. In *Advances in Neural Information Processing Systems (NIPS)*. Software available at <http://code.google.com/p/psvm>.
- Demmel, J., Grigori, L., Hoemmen, M., and Langou, J. (2012). Communication-optimal parallel and sequential QR and LU factorizations. *SIAM J. Sci. Comput.*, 34(1):206–239.
- Harchaoui, Z., Bach, F., Cappe, O., and Moulines, E. (2013). Kernel-based methods for hypothesis testing: A unified view. *Signal Processing Magazine, IEEE*, 30(4):87–97.
- Hinton, G., Deng, L., Yu, D., Dahl, G., rahman Mohamed, A., Jaitly, N., Senior, A., Vanhoucke, V., Nguyen, P., Sainath, T., and Kingsbury, B. (2012). Deep neural networks for acoustic modeling in speech recognition. *Signal Processing Magazine*.
- Huang, P.-S., Avron, H., Sainath, T., Sindhvani, V., and Ramabhadran, B. (2014). Kernel methods match deep neural networks on TIMIT. *Proc. of the IEEE International Conference on Acoustics, Speech, and Signal Processing (ICASSP)*.
- Krizhevsky, A., Sutskever, I., and Hinton, G. E. (2012). ImageNet classification with deep convolutional neural networks. In *Advances in Neural Information Processing Systems (NIPS)*.

- Le, Q., Sarlós, T., and Smola, A. (2013). Fastfood – Approximating kernel expansions in loglinear time. In *Proc. of the 30th International Conference on Machine Learning (ICML)*.
- Meng, X., Saunders, M., and Mahoney, M. (2014). LSRN: A parallel iterative solver for strongly over- or underdetermined systems. *SIAM Journal on Scientific Computing*, 36(2):C95–C118.
- Parikh, N. and Boyd, S. (2014). Block splitting for distributed optimization. *Mathematical Programming Computation*, 6(1):77–102.
- Pham, N. and Pagh, R. (2013). Fast and scalable polynomial kernels via explicit feature maps. In *Proceedings of the 19th ACM SIGKDD International Conference on Knowledge Discovery and Data Mining, KDD '13*, pages 239–247, New York, NY, USA. ACM.
- Rahimi, A. and Recht, B. (2007). Random features for large-scale kernel machines. In *Advances in Neural Information Processing Systems (NIPS)*.
- Schlkopf, B. and Smola, A. J. (2001). *Learning with Kernels: Support Vector Machines, Regularization, Optimization, and Beyond*. MIT Press.
- Socher, R., Perelygin, A., Wu, J., Chuang, J., Manning, C., Ng, A., and Potts, C. (2013). Recursive deep models for semantic compositionality over a sentiment treebank. In *In Proc. of the Conference on Empirical Methods in Natural Language Processing (EMNLP)*.
- Song, L., Boots, B., Siddiqi, S., Gordon, G., and Smola, A. (2013). Hilbert space embeddings of hidden Markov models. In *Proc. of the 30th International Conference on Machine Learning (ICML)*.
- Taijman, Y., Yang, M., Ranzato, M., and Wolf, L. (2014). DeepFace: Closing the gap to human-level performance in face verification. In *Proc. of the IEEE Conference on Computer Vision and Pattern Recognition (CVPR)*.
- Wahba, G. (1990). *Spline Models for Observational Data*. CBMS-NSF Regional Conference Series in Applied Mathematics.
- Yang, J., Sindhvani, V., Fan, Q., Avron, H., and Mahoney, M. (2014). Random Laplace feature maps for semigroup kernels on histograms. In *Proc. of the IEEE Conference on Computer Vision and Pattern Recognition (CVPR)*.

Yang, T. (2013). Trading computation for communication: Distributed stochastic dual coordinate ascent. In *Advances in Neural Information Processing Systems (NIPS)*.

Zhang, K., Peters, J., Janzing, D., and Scholkopf, B. (2011). Kernel based conditional independence test and application in causal discovery. In *Proc. 27th Intl. Conf. on Uncertainty in Artificial Intelligence (UAI)*.